IMPLEMENTATION OF A CREEP MODEL IN FLAC TO STUDY THE THERMOMECHANICAL RESPONSE OF SALT AS A HOST REPOSITORY MEDIUM—3RD PROGRESS REPORT

Prepared for

U.S. Nuclear Regulatory Commission
Contract No. NRC–HQ–12–C–02–0089

Prepared by

Biswajit Dasgupta
Goodluck Ofoegbu

Center for Nuclear Waste Regulatory Analyses
San Antonio, Texas

August 2018

CONTENTS

FIGURES

TABLES

ACKNOWLEDGMENTS

This report was prepared to document work performed by the Center for Nuclear Waste Regulatory Analyses (CNWRA®) for the U.S. Nuclear Regulatory Commission (NRC) under Contract No. NRC–HQ–12–C–02–0089. The activities reported here were performed on behalf of the NRC Office of Nuclear Material Safety and Safeguards, Division of Spent Fuel Management. The report is an independent product of CNWRA® and does not necessarily reflect the view or regulatory position of NRC. The authors gratefully acknowledge the technical and editorial reviews of David Pickett and the programmatic review of Gordon Wittmeyer, and the assistance of Arturo Ramos in preparing this report.

QUALITY OF DATA, ANALYSES, AND CODE DEVELOPMENT

DATA: All CNWRA-generated original data contained in this report meet the quality assurance requirements described in the CNWRA Quality Assurance Manual.

ANALYSES AND CODES: The computer software code FLAC® Versions 7.0 (Itasca Consulting Group, 2011) and 8.0 (Itasca Consulting Group, 2016) was used in the analyses contained in this report. FLAC is commercial software controlled under Technical Operating Procedure (TOP)–018, Development and Control of Scientific and Engineering Software. Documentation of the calculations can be found in Scientific Notebook 1237E (Dasgupta and Ofoegbu, 2017).

REFERENCES

Dasgupta, B. and G. Ofoegbu. "Numerical Implementation, Testing, and Use of a Constitutive Model for Mechanical Behavior of Salt." Scientific Notebook No. 1237E. San Antonio, Texas: Center for Nuclear Waste Regulatory Analyses. 2017.

Itasca Consulting Group, Inc. "FLAC Fast Lagrangian Analysis of Continua." Version 8. Minneapolis, Minnesota: Itasca Consulting Group, Inc. 2016.

_____. "FLAC Fast Lagrangian Analysis of Continua." Version 7. Minneapolis, Minnesota: Itasca Consulting Group, Inc. 2011.

1 INTRODUCTION

1.1 Background

This report documents continued studies conducted on behalf of the U.S. Nuclear Regulatory Commission (NRC) to assess the mechanical behavior of salt rock at the Waste Isolation Pilot Plant (WIPP) in the context of generic geologic disposal of high-level radioactive waste. An approach for modeling the mechanical behavior of salt rock was developed, implemented for use in FLAC® (Fast Lagrangian Analysis of Continua; Itasca Consulting Group, 2016) as a user-defined material model, and used to model salt rock behavior for heated and ambient conditions at WIPP. This report documents analyses performed to evaluate the modeling approach and identify needed changes. In previous reports on the salt rock modeling study, Ofoegbu and Dasgupta (2015, 2017) described the user-defined material model as consisting of a model for creep deformation based on a European Commission salt model known as FZK-INE (European Commission, 2007) and a model for plastic deformation developed in-house by the authors. The reports also describe modeling of two in-situ experiments on time-dependent deformation of underground openings in salt rock conducted previously at WIPP.

As discussed in Ofoegbu and Dasgupta (2017), several deformation mechanisms could contribute strain increments in salt rock, such as Δe_{ij}^{E}, Δe_{ij}^{P}, Δe_{ij}^{Th}, Δe_{ij}^{D}, and Δe_{ij}^{C}, due to elastic, plastic, thermal-expansion, damage, and creep deformation mechanisms, respectively. A key assumption in developing stress-strain relationships for the material model is that the strain contributions of the various deformation mechanisms are separable and additive. The assumption is based on common practice and is fundamental to modeling generalized stress-strain relationships (e.g., Desai and Siriwardane, 1984; p. 223). Separability implies that each strain contribution can be modeled separately based on an understanding of the associated deformation mechanism. Also, additivity implies the various strain contributions can be added to obtain the total strain increment. The authors developed a model for plastic strain and damage based on the plasticity theory and a model for creep strain based on the aforementioned FZK-INE model. However, Ofoegbu and Dasgupta (2017) found the creep model inadequate to account for the inelastic response of salt rock around the underground openings. Therefore, Ofoegbu and Dasgupta (2017) developed a plasticity model that runs in combination with the creep model.

The creep model includes contributions due to transient creep and steady-state creep. Although the FZK-INE model also includes a volumetric strain component described as damage creep, the volumetric strain aspect was removed from the creep model. Inelastic volumetric strain is instead modeled through dilation in the plasticity model. Also, analysis by the authors showed that the contribution of transient creep alone represents the creep behavior adequately. Therefore, the authors focused on evaluating the effects of the three transient creep parameters a_0, a_1, and a_2, as described in Ofoegbu and Dasgupta (2017, Chapter 2).

The plasticity model is defined in terms of four parameters: (i) the cohesive strength parameter q_0 and (ii) frictional strength parameters $\mu_{\max}$, $\mu_{\min}$, and d_c. As described in Ofoegbu and Dasgupta (2017, Section 3.1.3), the plasticity model was used to model the WIPP underground openings based on a starting guess of $q_0 = 2.5$ MPa, $\mu_{\min} = 0.1$, $\mu_{\max} = 2.0$, and $d_c = 10$. The values were estimated from test data in Hunsche and Hampel (1999), because the authors did not find any supporting WIPP salt data for the plasticity model.

1.2 Current Report

The authors performed calculations in 2017 to model rock behavior around the WIPP underground openings Room D (ambient temperature conditions) and Room B (heated conditions) using FLAC with the user-defined material model (described in Section 1.1) that includes elastic, creep, and plastic deformation models. The calculations used a modified approach for simulating rock excavation for the room as described in Chapter 2. The focus of this report is to determine the values of the transient creep parameters a_0, a_1, and a_2 (Ofoegbu and Dasgupta, 2017) needed to match the measured rock convergence around the openings. Additionally, the ratio of the horizontal to vertical in situ stress was also modified to determine an appropriate value for modeling the underground openings. Assuming the rock stratigraphy as a homogeneous continuum medium, the calibrated parameters from the Room D simulation under ambient conditions were used for heated Room B. In a separate model, simulation of Room D was studied with explicit representation of clay seams as a contact interface.

Simulation results for Rooms D and B show that the shape and the trend of calculated convergence are similar to the measured convergence (Chapter 2). However, the magnitude of the calculated convergence history is different from the magnitude of the measured history, especially for longer times. Based on the observed response of the clay model, modeling the clay seam as an interface did not improve the calculated convergence.

The authors expect that calculated convergence histories that match the measured convergence histories can be obtained by modifying values of the plasticity model parameters and developing a model to represent the effects of plastic deformation on the creep parameters. First, values of the plasticity model parameters (cohesive strength parameter q_0 and frictional strength parameters $\mu_{\max}$, $\mu_{\min}$, and d_c) appropriate for the WIPP underground openings could be different from the starting values applied in the calculation. Second, the authors expect the creep resistance (modeled through the creep parameters a_0, a_1, and a_2) to be affected by inelastic strain, similar to the effect of the plasticity model parameters on shear resistance [as described in Ofoegbu and Dasgupta (2017, Section 3.1.2)]. Therefore, the effects of inelastic strain on the creep parameters need to be accounted for in the model in order to perform a meaningful evaluation of the effects of the plasticity model parameters on calculated convergence. The scope of work in 2017 could not accommodate the effort needed to modify the material model to account for the effects of inelastic strain on the creep parameters. Consequently, the effects of modifying values of the plasticity model parameters on calculated convergence have not been evaluated.

2 NUMERICAL MODELING OF PUBLISHED IN SITU TESTS CONDUCTED AT THE WASTE ISOLATION PILOT PLANT (WIPP)

2.1 WIPP In-situ Experiment

The coupled salt creep and plasticity constitutive model developed in this project and implemented in the geomechanical computer code FLAC was used to model in-situ experiments conducted previously at WIPP. The experiments consisted of long term measurements of rock convergence around two underground openings constructed in bedded salt—test facility Rooms B and D. As described in Rath and Argüello (2012), Rooms B and D were located at the same general location and horizon at WIPP. Room D remained at ambient temperature conditions, while Room B was subjected to applied thermal loads using embedded heaters below the floor. The rooms are 5.5 m [16.4 ft] wide, 93.3 m [306.0 ft] long, and 5.5 m [16.4 ft] high, located at a depth of 646 m [2,119 ft] below the ground surface. The subsurface stratigraphy at the location of the rooms consists mainly of layers of halite and argillaceous halite interrupted by several horizontal clay seams (Rath and Argüello, 2012, Figure 3-1).

The closure histories for Rooms B and D based on field measurement data are shown in Figure 2-1. In the absence of numerical data for the closure measurements, the data for the plots in Figure 2-1 were obtained by digitizing the Rooms B and D closure history plots in Rath and Argüello (2012). As shown in Figure 2-1, the heaters in Room B were turned on after about 300 days, prior to which the room was at an ambient state, whereas Room D was under ambient conditions throughout the experimental period. During the ambient period, the plots in Figure 2-1 show that closure was slightly greater in Room B than in Room D.

2.2 Model Geometry and Initial and Boundary Conditions

Site specific data and loading conditions used in the model were obtained from Rath and Argüello (2012). Two-dimensional (2-D) plane strain models were developed using FLAC at the mid-section of the rooms. The test section of unheated Room D is in the middle 74.4 m [244.0 ft] of the 93.3 m [306.0 ft] long room. The heated Room B has heaters placed below the floor, symmetric with the center line of the room. The heaters, which simulate the effects of heat-generating radioactive waste canisters, were placed at regular intervals {center to center spacing 1.52 m [5 ft]} in bore holes in the middle 24.4 m [80.0 ft] of the 93.3 m [306.0 ft] long room (Rath and Argüello, 2012). Additional heaters were placed symmetrically on either end of the room. The heater system provides a uniform temperature distribution along the entire length of the test section. Because of these symmetries, 2-D models are appropriate for studying the thermal and mechanical responses of the room in the experiments.

The experimental test rooms were constructed in bedded stratigraphy of natural salt separated by several thin horizontal clay seams. The stratigraphy of the rock and the location of clay seams around Room D is based on Rath and Argüello (2012). Because the two rooms have identical geometry and essentially identical geology, Room D was used for simulation of rock deformation under ambient and heated conditions. Two types of models were developed: (i) a continuum model in which the clay seams were not incorporated and (ii) another in which the clay seams were explicitly modeled as interfaces. Several analysis cases of the continuum Room D (nonheated) model were performed to determine appropriate material model parameters. The calibrated material properties were used for both the heated and the clay seam models.

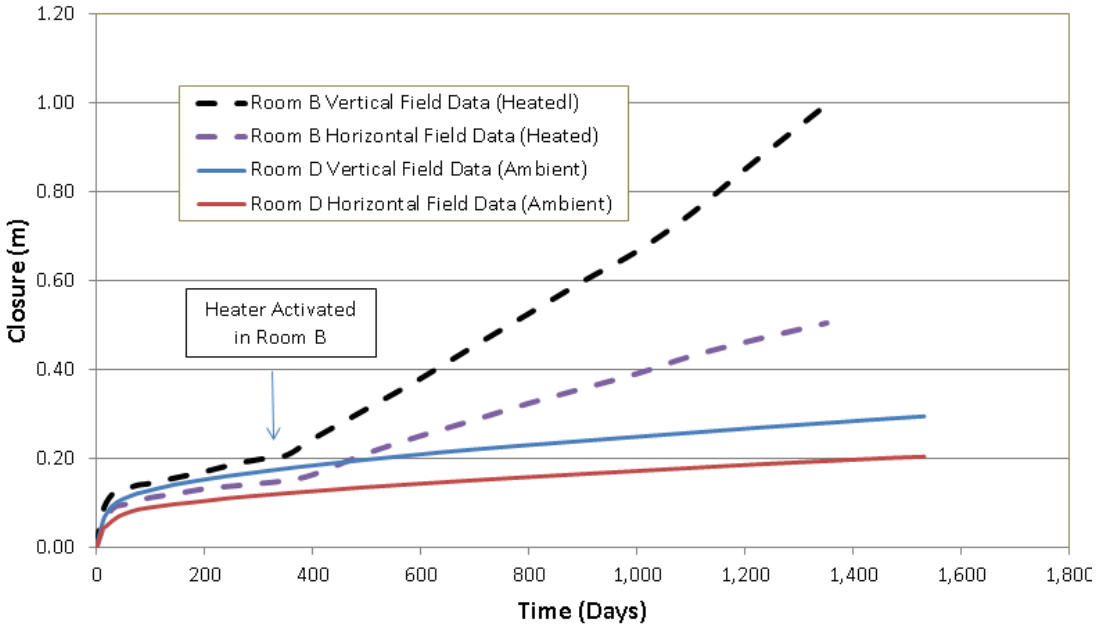

Figure 2-1. Vertical and Horizontal Closure History for Room B (Heated) and Room D (Ambient) at WIPP.

The model geometries for the Rooms B and D continuum analyses are shown in Figure 2-2 and the Room D model with clay layers is shown in Figure 2-3. Half of the room section was modeled using a vertical plane of symmetry along the center line of the room. The initial vertical stress (σ_v) varies linearly with depth and the initial horizontal stress (σ_h) was varied from 1.0 to 1.5 times the vertical stress. The mechanical boundary conditions are shown in Figure 2-2(a). The horizontal displacement is restrained on vertical boundaries. A uniform pressure of 13.57 MPa, in accordance with the overburden pressure (Rath and Argüello, 2012), was applied on the top boundary and a roller boundary was applied to the bottom horizontal boundary.

The thermal boundary conditions are shown in Figure 2-2(b). The initial temperature of the model is 300 K [26.9 °C, 80.3 °F] (ambient temperature of the room) and the model boundaries are held at the initial temperature through the simulation period; temperature dependence with depth below ground level was not included. This assumption is reasonable because the geothermal gradient over a relatively short model extent in the vertical direction has a minimal effect on the thermal-mechancial response of the model. The heater is placed along the plane of symmetry. The heater location and length are shown in Figure 2-2(b), based on Rath and Argüello (2012). Similar to Rath and Argüello (2012), the heat load exponentially decayed with time and the thermal conductivity of salt was modeled as a nonlinear function as described in Ofoegbu and Dasgupta (2015).

The modeling sequences used for Room D included first development of a static stress field using initial stress conditions. After the initial consolidation of the model, rock excavation of the room was simulated by deleting the zones representing the room area. However, to avoid spurious stress development in the model from instantaneous excavation, the traction along the excavation boundary was reduced gradually to zero in several steps. A user-defined routine was implemented in FLAC to control the traction reduction. The vertical and horizontal convergences were monitored in the model. In the Room D model, creep was simulated for 1,400 days after excavation. The ambient temperature for Room D, which remained constant throughout the analysis, was assumed to be 300 K [26.9 °C, 80.3 °F].

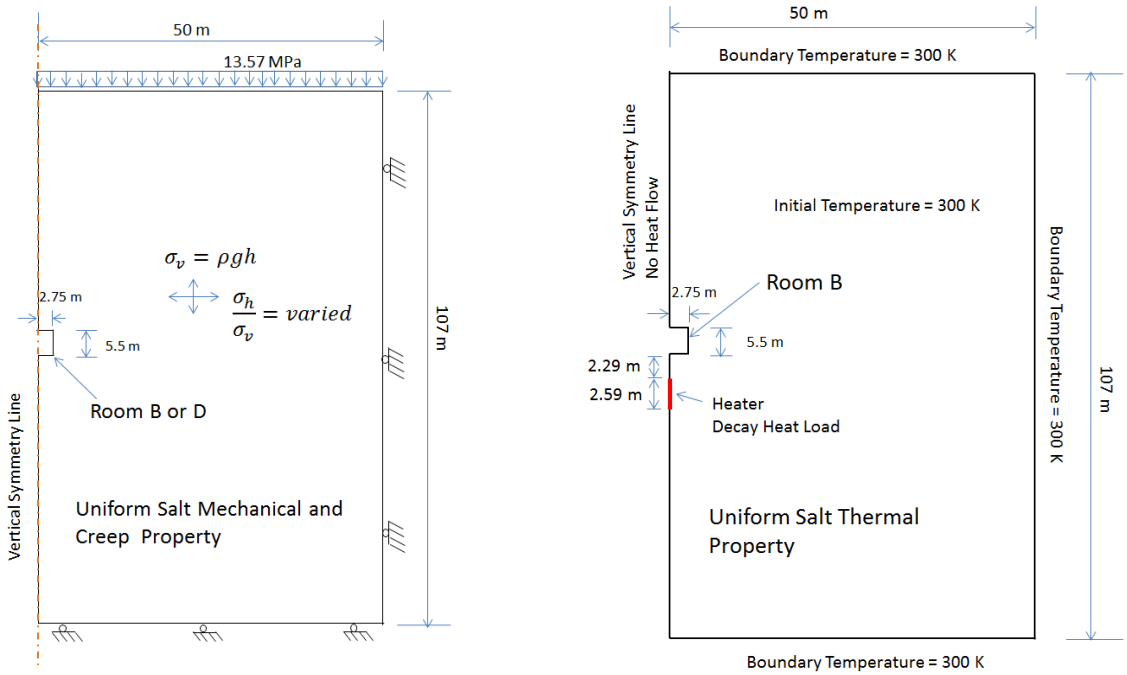

Figure 2-2. Model Geometry and Boundary Conditions for (a) Mechanical and (b) Thermal Models (1.0 MPa = 145.03 psi, 1.0 m = 3.28 ft)

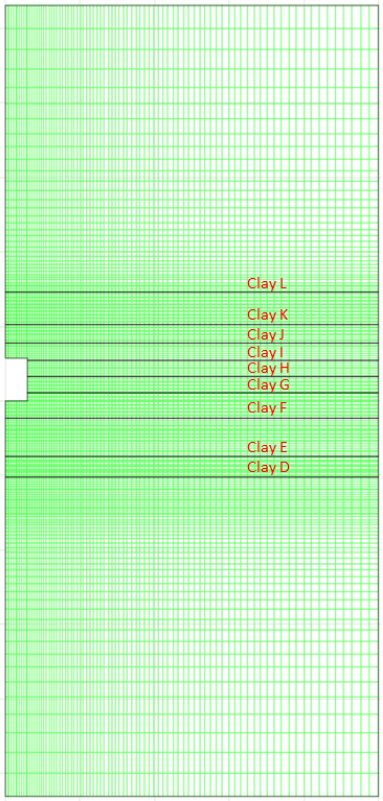

Figure 2-3. FLAC Model Geometry of Room D with the Clay Layers Delineated as Dark Lines

For the heated Room B simulation, one-way coupling of thermal and mechanical responses was employed as described in Ofoegbu and Dasgupta (2015). A thermal analysis was first performed using FLAC to generate the temperature of the model-discretized zones for the heat load applied at the heater location for 1,000 days. The computed temperature was saved at specific intervals during the thermal simulation for application in the mechanical model. The thermal analysis discussed in Ofoegbu and Dasgupta (2015) was used in the mechanical calculations. Because of the initial steep gradient of heat load, the zone temperature from the thermal analyses was saved at smaller intervals initially and the interval was increased when the heat load exponentially decayed with time. The mechanical model was initiated in a similar way as for the Room D model, but the creep analysis at the ambient temperature of 300 K [26.9 °C, 80.3 °F] was performed for 320 days. The zone temperature data were provided as inputs into the mechanical model at specific times to ensure the creep and thermal times were synchronized.

The Room D model with clay layers is shown in Figure 2-2. Clay layers D to L closer to the excavated area were incorporated in the model based on the stratigraphy obtained from Rath and Argüello (2012). The clay seams noted in Rath and Argüello (2012) are primarily local "horizontal concentrations of disseminated clay stringers." Therefore, the seams were incorporated in the models as contact surfaces with prescribed clay properties. Rath and Argüello (2012) assumed the contact to be frictional with a coefficient of friction equal to a value of 0.2 (or friction angle as 12°). Interfaces between grids can be modeled explicitly in FLAC. These interfaces are planes upon which slip and/or separation is allowed. Interfaces are characterized by Coulomb sliding and/or tensile separation. Interface properties in FLAC consist of friction, cohesion, dilation, normal and shear stiffness, and tensile strength.

2.3 Material Model Options

The parameter values are described in this section and were used in different analysis cases as described in Section 2.4.

2.3.1 Linear Elastic Parameters

The density and linear elastic parameter values for halite used in the modeling are similar to the values in Table 2-1 of Ofoegbu and Dasgupta (2015) and are given as follows [1.0 Kg/m^3 = 0.062 lb/ft^3 and 1 MPa = 145 psi]:

Density ρ = 2,300 Kg/m^3
Young's modulus $E = 6.27 \times 10^3$ MPa
Poisson's ratio $\nu = 0.45$

2.3.2 Creep Parameters

The parameters used for the creep model in Table 2-1 of Ofoegbu and Dasgupta (2015) are used in this analysis. Note that the dilatant creep coefficients and the exponent were not used, because the material deformation due to material damage is modeled using the plasticity model (Ofoegbu and Dasgupta, 2017). The following creep parameters are used in the analysis:

Activation energy $Q = 54.21$ kJ/mol
Universal gas constant $R = 8.31 \times 10^{-3}$ kJ/(mol.K)
Structural factor (for steady state and dilatant creep) $A = 0.18014$ MPa^{-5}/day
Transient creep coefficients a_0, a_1, and a_2 are given in Tables 2-1 and 2-2.

Exponent for transient creep $n_t = 5.0$
Exponent for steady state creep n_s = 5.0
Initial porosity of salt rock $\eta_0 = 2.0 \times 10^{-4}$

2.3.3 Nonlinear Elastic Parameters

The nonlinear elastic model based on a dilation-dependent bulk modulus is described in Chapter 3 of Ofoegbu and Dasgupta (2017). The parameters and the values assumed are given as follows:

Elastic (or initial) bulk modulus $K_E = 2.09 \times 10^4$ MPa
Minimum compressibility coefficient $\kappa_{\min} = 0.05$
Maximum compressibility coefficient $\kappa_{\max} = 2.0$
Decay parameter for compressibility coefficient $d_k = 100$
Minimum (i.e., initial) specific volume $v_{\min} = 1.002$

2.3.4 Plasticity Model Parameters

The salt plasticity model described in Chapter 3 of Ofoegbu and Dasgupta (2017) requires five parameters. Following are the parameter and values used in all model cases where plasticity is used.

Cohesive strength parameter, $q_0 = 10$ MPa
Yield function parameters, $k_0 = 0.0$, $k_1 = 0.024$
Maximum shear resistance coefficient, $\mu_{\max} = 2.0$
Minimum shear resistance coefficient, $\mu_{\min} = 0.1$
Shear resistance decay coefficient, $d_c = 10$

2.3.5 Clay Seam Parameters

Clay seams are represented as relatively weak interfaces between layers of salt rock. The interface properties required in the model and the parameter values are:

Friction angle = $12°$ and $20°$
Cohesion = 0.01 MPa and 0 MPa
Tensile strength = 0.001 MPa and 10.0 MPa
Normal stiffness = 1.2×10^5 MPa/m
Shear stiffness = 1.2×10^5 MPa/m

2.3.6 Thermal Parameters

The thermal parameters used in the Room B analysis are defined in Table 2-1 of Ofoegbu and Dasgupta (2015).

Thermal expansivity, $\alpha = 4.2 \times 10^{-5}\ 1/K$
Thermal conductivity, $\lambda = \lambda_{300}(300/T)^{\gamma}$,
where $\lambda_{300} = 4.32 \times 10^5\ (J/(m.day.K)$, $\gamma = 1.14$, and T is absolute temperature in Kelvin (K).

2.4 Analysis Cases for WIPP Rooms

Modeling convergence of WIPP Rooms consists of three parts: (1) continuum analysis of unheated Room D without clay seams, (2) analysis for Room D with clay seams incorporated, and (3) thermal analysis of heated Room B. The Rooms B and D WIPP experiments differ only in that a thermal load was applied in Room B, whereas Room D was held at ambient temperature.

2.4.1 Room D: Continuum Analysis

The Room D analysis case used nonlinear elasticity, creep, and plasticity models. Elastic deformation was represented using the nonlinear elastic model, creep was represented using constant parameters, and the plasticity model was introduced to account for instantaneous inelastic deformation that is beyond the scope of creep modeling. Such inelastic deformation includes interparticle movements driven by mechanisms that are similar to creep but occur instantaneously, could progress to observable material failure, and are controlled by stress and material deformation history. Therefore, several analysis cases of Room D were performed to choose a material model combination and in-situ stress ratio that match with the field measurement. The calibrated model parameters was used for the Room B simulation.

Table 2-1 shows the simulation cases studied for Room D. As can be seen from the table, the transient creep parameter a_0 was held constant for each case during the simulation. Ofoegbu and Dasgupta (2017) investigated contributions to convergence due to rock creep from small deviatoric stress conditions. The investigation was based on describing the transient creep parameter a_0 as a function of deviatoric stress, represented through a nondimensional stress ratio $R_s = q/p$, where q and p are the deviatoric stress and effective mean stress, respectively. Ofoegbu and Dasgupta (2017) concluded that although increased creep rates from small deviatoric stress conditions resulted in increased convergence, the shape of the calculated convergence history departed from the shape of the measured history enough to indicate that the calculated effect is not consistent with rock behavior around the openings. Therefore, variation of a_0 with R_s was not included in this study. The parameter values for a_1, and a_2 in Table 2-1 were obtained from sensitivity analyses in order to best fit the convergence curve during the transient creep response.

The parametric variation of transient-creep parameter a_0 (Table 2-1) used in the simulation ranges from the lowest value 0.008 to the highest value 0.05, with intermediate values of 0.01, 0.02, and 0.03. Only two parameter values were used for a_1, 1,750 and 2,000, while for a_2 only one value, 0.375, was used. The horizontal to vertical in-situ stress ratios considered in these analyses were 1.0, 1.25, 1.3, and 1.5. In the calculated convergence histories shown in Figures 2-4 to 2-9, closure shape, trend, and magnitude were evaluated to find the cases that are comparable to the field data. The closure measurements, as discussed in Section 2.1, were obtained by digitizing the plots from Rath and Argüello (2012). The digitized data set referred to as Field Data-1 had a nonzero value at time zero. The Field Data-2 set was developed from Field Data-1 by subtracting the initial value at time $t = 0$. The calculated closure (i.e., convergence) histories were compared with Field Data-1 and Field Data-2.

The vertical and horizontal closure histories for all cases are plotted in Figures 2-4 and 2-5. As the figures show, the simulation cases CONM-3, -6, -8 and -10 were stopped because the convergence magnitude significantly deviated from the measured data within 300 simulated days. The closure history for CONM-4 shows that although the horizontal history is fairly close to the measured plots (Figure 2-5), the vertical closure was significantly under-predicted

Table 2-1. Simulation Cases for Room D Continuum Model (CONM)				
Case	a_0	a_1	a_2	σ_h/σ_v
CONM-1	0.008	1,750	0.375	1.5
CONM-2	0.01	1,750	0.375	1.5
CONM-3	0.01	1,750	0.375	1.0
CONM-4	0.02	1,750	0.375	1.0
CONM-5	0.05	1,750	0.375	1.0
CONM-6	0.01	1,750	0.375	1.25
CONM-7	0.02	1,750	0.375	1.25
CONM-8	0.05	1,750	0.375	1.25
CONM-9	0.02	1,750	0.375	1.3
CONM-10	0.03	1,750	0.375	1.3
CONM-11	0.03	2,000	0.375	1.3

Notes
1. a_0, a_1, and a_2: transient creep parameters
2. σ_h = horizontal in-situ stress; and σ_v = vertical in-situ stress

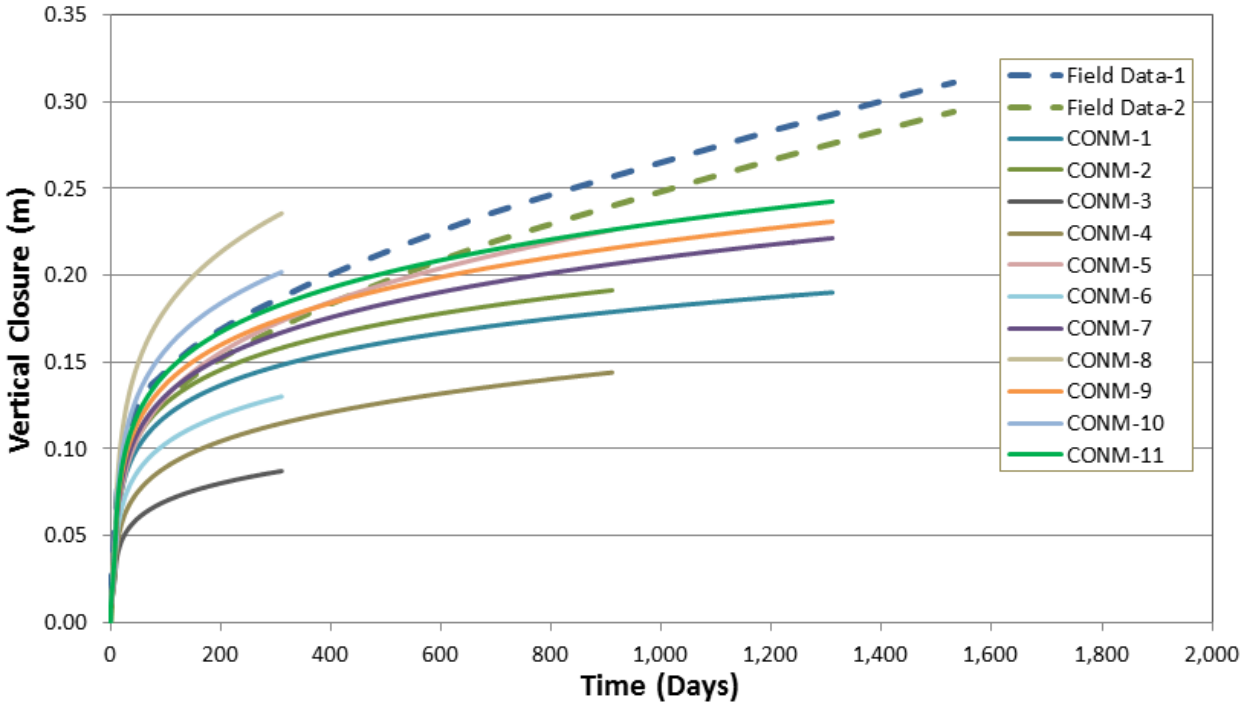

Figure 2-4. Vertical Closure Compared with Field Data: All Cases

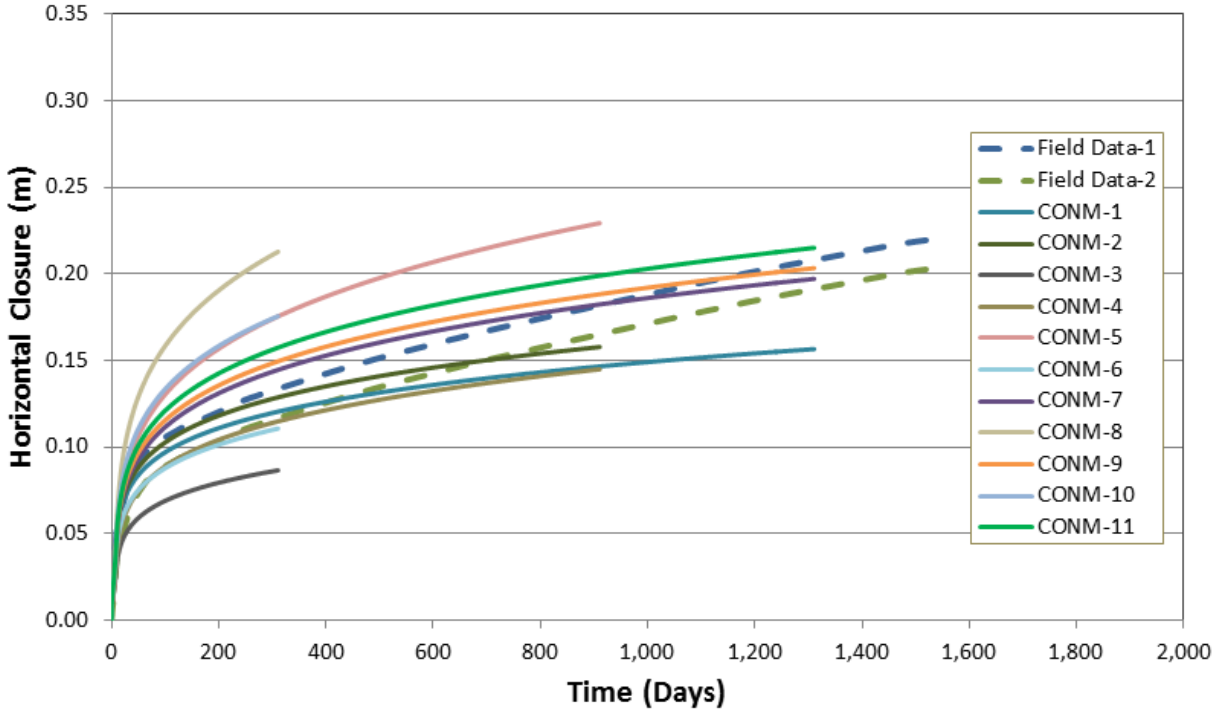

Figure 2-5. Horizontal Closure Compared with Field Data: All Cases

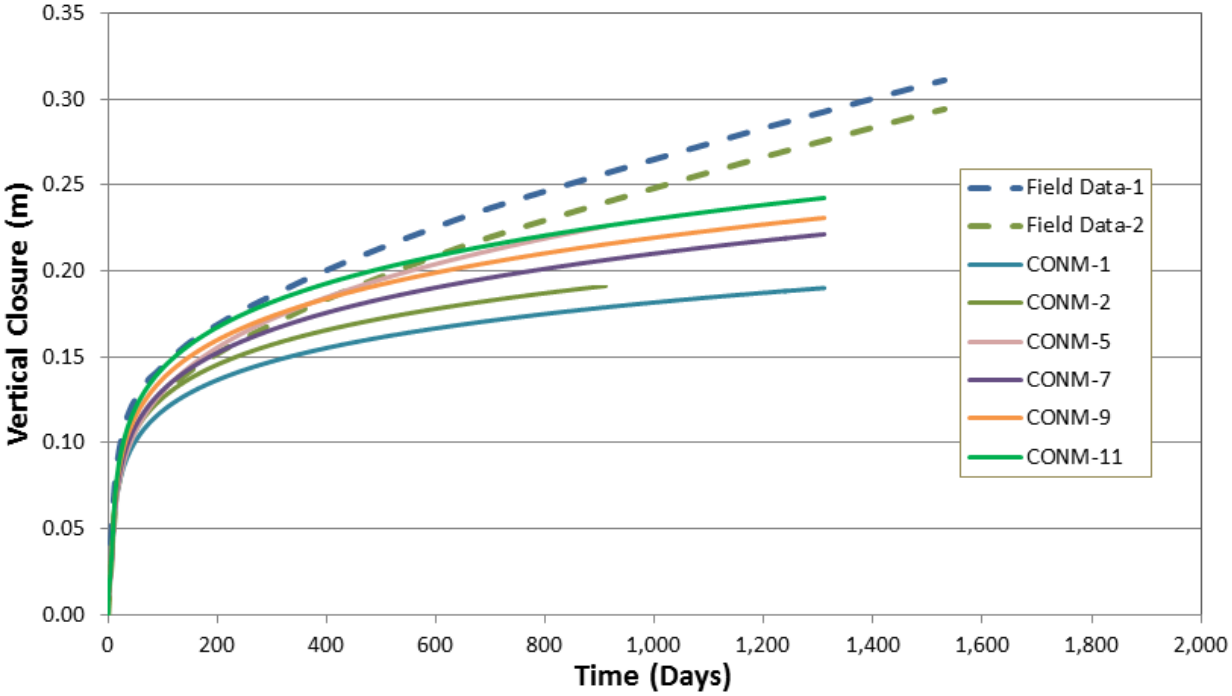

Figure 2-6. Vertical Closure Compared with Field Data: Cases Screened Out That Significantly Deviated from Measured Values

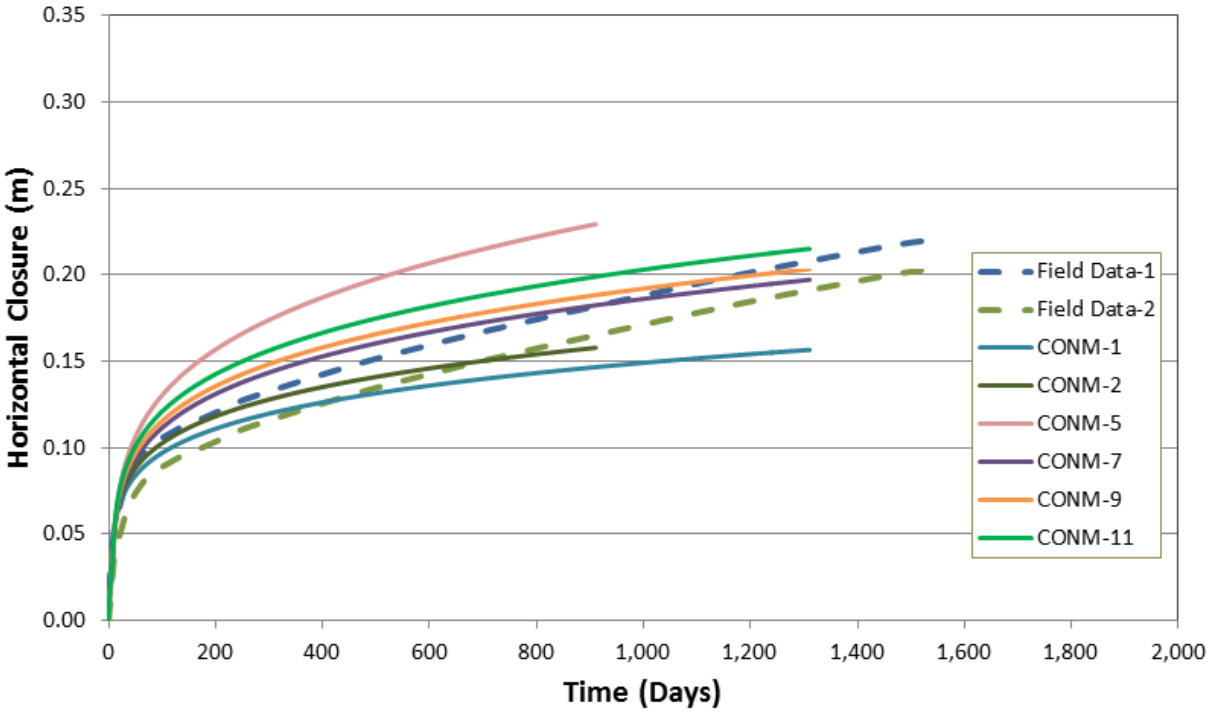

Figure 2-7. Horizontal Closure Compared with Field Data: Cases Screened Out That Significantly Deviated from Measured Values

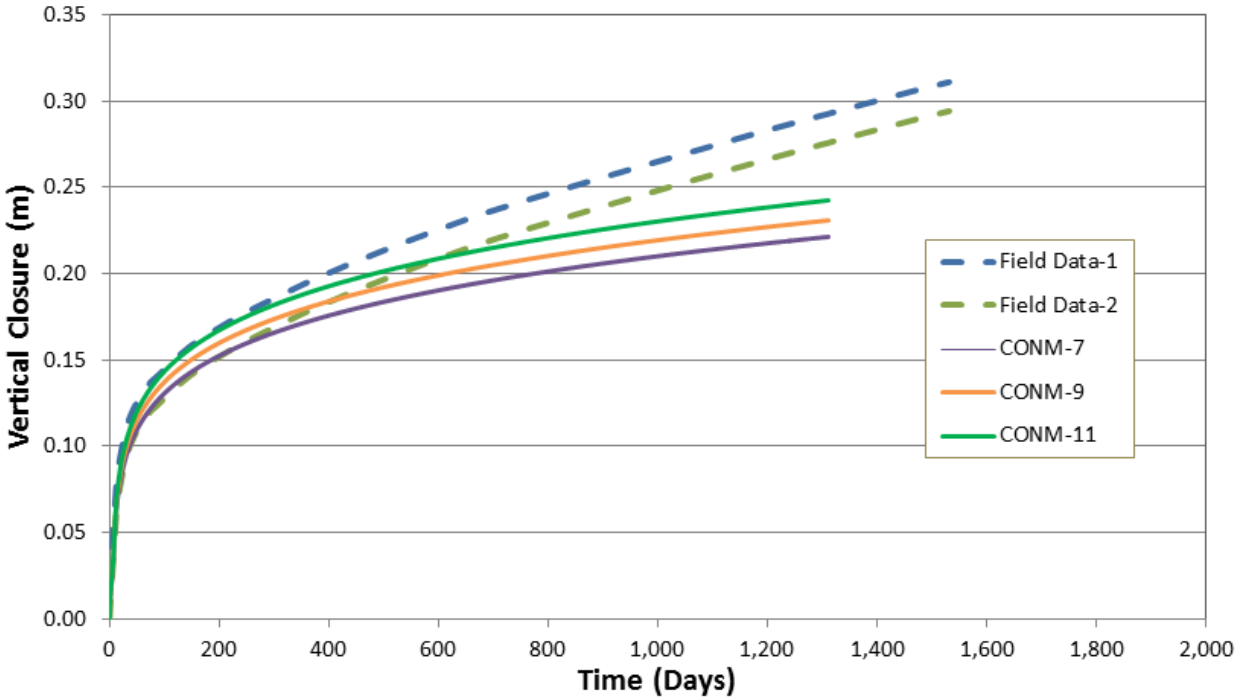

Figure 2-8. Vertical Closure Compared with Field Data: Cases Considered Comparable to Measured Data

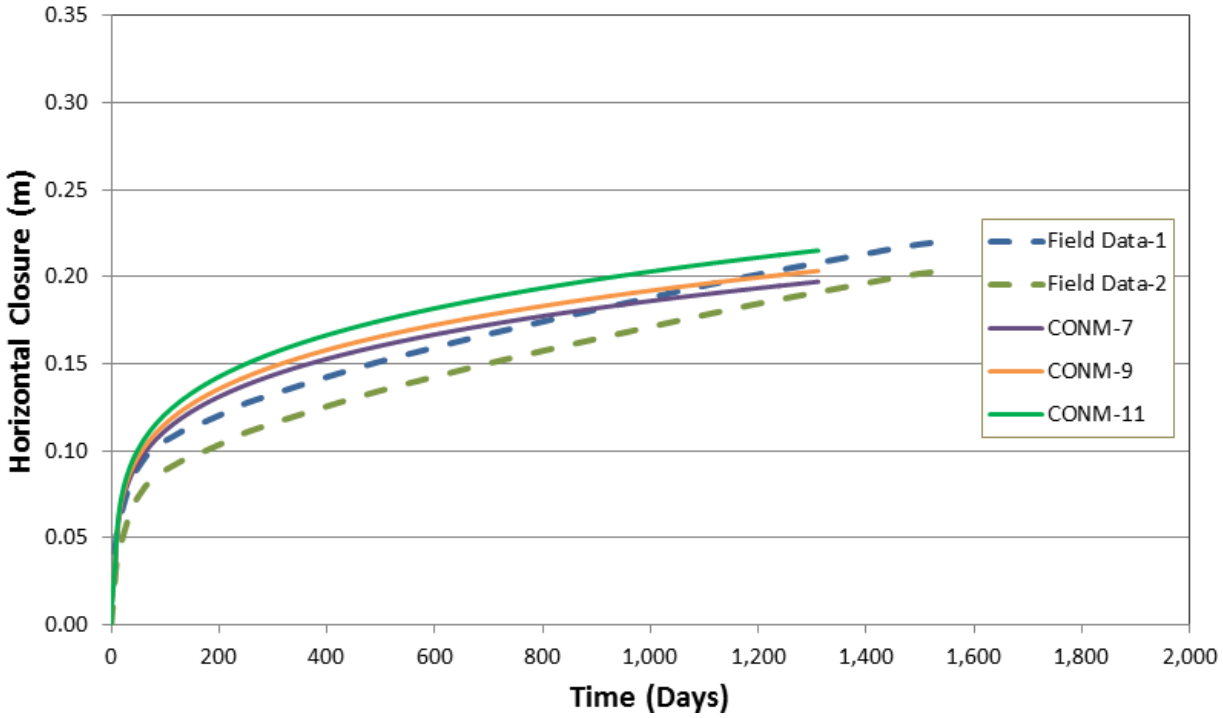

Figure 2-9. Horizontal Closure Compared with Field Data: Cases Considered Comparable to Measured Data

(Figure 2-4). Figures 2-6 and 2-7 show the convergence plot with cases CONM-3, -4, -6, -8 and -10 eliminated from further consideration. It can be seen that the vertical closure for simulation case CONM-5 is within the range of the measured data (Figure 2-6), but horizontal convergence is predicted higher (Figure 2-7). Similarly, cases CONM-1 and CONM-2 can be considered to be within the range of horizontal closure in Figure 2-7, but they under-predicted the vertical closure as seen in Figure 2-6. Thus CONM-1, -2, and -5 were not considered further for comparison with measured data. In summary, the following cases were eliminated based on visual observation of the plots: (1) all cases with σ_h/σ_v equal to 1.5 or 1.0 (CONM-1 to -5); and (2) all cases with a_0 = 0.05 and 0.01 (CONM-2, -3, -5, -6 and -8).

Observing the closure histories in Figures 2-8 and 2-9, simulation cases CONM-7, -9 and -11 compare best with the measured data. For vertical convergence the predicted closure compares well up to 500 days. Thereafter, the long duration trend is predicted lower than the measured data. Horizontal closure is generally seen to be predicted higher than measured values for these cases. For the selected cases, calculated vertical convergence at 1,300 days is within 75–80 percent of the measured convergence (Field Data-1). Analyzing the simulation cases, it is seen that a_0 varies between 0.02 and 0.03 and a_1 varies between 1,750 and 2,000, while a_2 is constant at 0.375. It can also be seen that σ_h/σ_v varies between 1.25 and 1.3. This appears reasonable for an in situ stress scenario at the excavation horizon located at 640 m [2,100 ft] below the ground surface. Parameter values for CONM-9 were used for further simulation for heated Room B and the clay seam model.

Simulation results for Room D show that the shape and the trend of the calculated convergence are similar to the measured convergence, but the magnitude of the calculated convergence history is different from the magnitude of the measured history. The transient parameters have been adequately characterized and calibrated for the WIPP salt rock, and the authors expect that calculated convergence histories can be further improved by: (a) modifying the values of

plasticity parameters and (b) introducing strain-based coupling between creep and plasticity as explained in Chapter 1.

2.5 Room D: Clays Seams Included as Interfaces

In this analysis case, salt rock is represented as layers with material properties as described in Section 2.2. To represent clay seams, the layer interfaces were modeled as weak relative to the salt rock layers. The interface properties are as described in Section 2.3.5. The mechanical effects on convergence are sensitive to both stiffness and strength properties of the clay layer. Since these properties are not directly measurable in the laboratory, they are assumed based on available information in the literature and further calibrated based on the expected mechanical response. Simulation cases for Room D with clay seams incorporated are listed in Table 2-2; the calculated vertical and horizontal closure histories are shown in Figures 2-10 and 2-11, respectively. In one case (CSM-1), the interface properties were assumed to have strength to inhibit slip or opening. As expected, the model responded like the continuum rock mass model and the convergence profile is similar to CONM-9. In the other cases (CSM-2 and CSM-3), the layer properties were assumed to be very weak and the model showed very high convergence compared to the field measurements. These two extreme cases showed that the modeling approach is reasonable. However, representing a clay seam as a contact interface may not be appropriate. For future studies, the clay seams can be modeled as thin layers rather than interfaces, and a material model based on coupled creep and plasticity can be applied.

2.6 Room B: Heated Experiment

The thermal analysis of heated Room B is described in Section 2.3 and the thermal parameters used are given in Section 2.3.6. The temperature contours from a FLAC thermal analysis at the end of 1,000 days are shown in Figure 2-6 of Ofoegbu and Dasgupta (2015) and the temperature versus time plots at specific locations below the floor of the excavation are shown in Figure 2-8 of Ofoegbu and Dasgupta (2015). A total of 46 sets of zone temperatures were saved from the thermal analyses. Because of the steep gradient of the initial heat load, the temperature was saved at 4.8-hour intervals for the first day, 1-day intervals up to the 10th day, 2-day intervals up to the 20th day, 5-day intervals up to the 50th day, 10-day intervals up to the 100th day, 50-day intervals to the 500th day, and 100-day intervals up to the 1,000th day. The material model combination for analysis case CONM-9 (Table 2-1) was used to conduct the mechanical analysis of the heated Room B experiment, because CONM-9 resulted in vertical and horizontal convergences that were closest to the field measurements in unheated Room D. The model was executed under ambient conditions up to 320 days, after which thermal loading was applied. The material model combination consisted of nonlinear elasticity, plasticity, and creep (with $a_0 = 0.02$, $a_1 = 1750$, and $a_2 = 0.375$) with a horizontal to vertical stress ratio of 1.3. The calculated vertical and horizontal closures for the heated conditions are compared with the measured convergence from Room B in Figures 2-12 and 2-13. The history plots show an increase in convergence with application of thermal loading after the ambient period, consistent with the measured convergence history. However, during the period of heating, the calculated magnitude for both vertical and horizontal convergence is smaller than the measured magnitude. Comparing Figures 2-12 and 2-13, the model results for horizontal closure performed better than for vertical closure.

Table 2-2. Simulation Cases for Room D Discontinuum Clay Seam Model (CSM)							
Case	a_0	a_1	a_2	σ_h/σ_v	c $[MPa]$	ϕ $[degrees]$	Tensile Strength $[MPa]$
1 CSM-1	0.02	1,750	0.375	1.3	0.02	22	10.0
2 CSM-2	0.03	1,750	0.375	1.3	0.0	12	10.0
3 CSM-3	0.03	1,750	0.375	1.3	0.0	12	0.001

Notes
1. a_0, a_1, and a_2: transient creep parameters
2. σ_h = horizontal in-situ stress; and σ_v = vertical in-situ stress
3. c = Cohesion; and ϕ = Friction angle
4. $1.0\ MPa = 145.03\ psi$

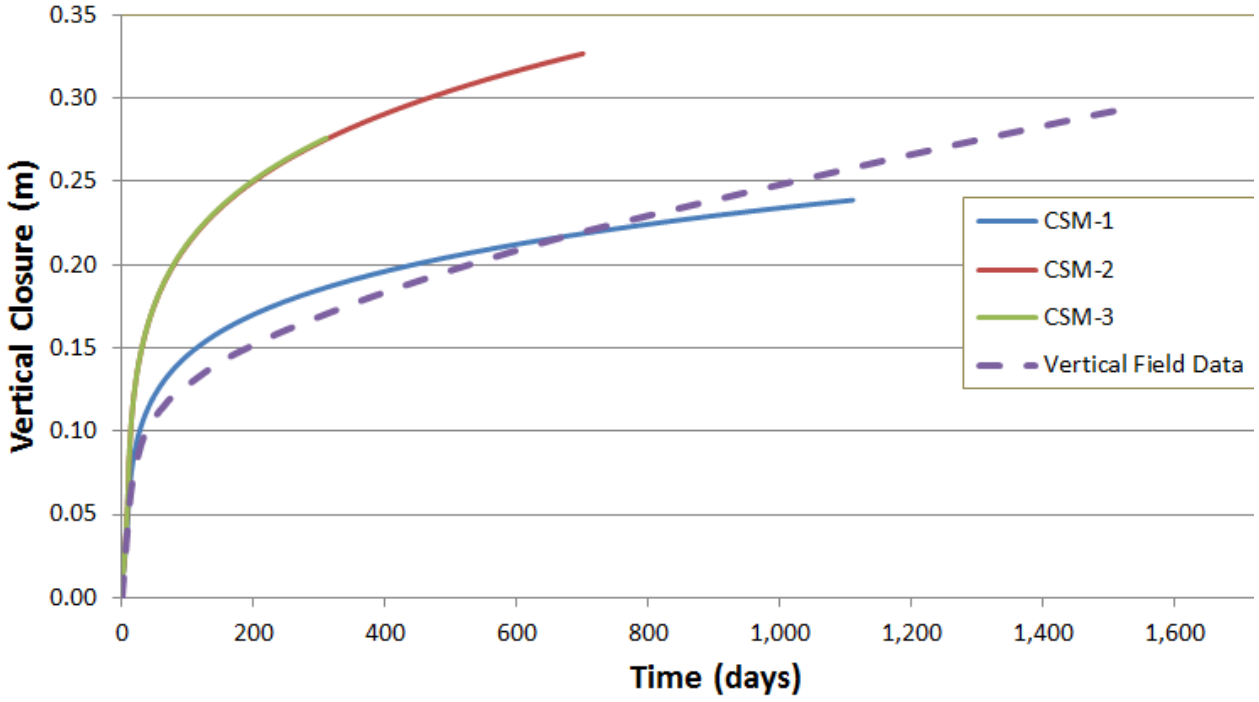

Figure 2-10. Vertical Closure History for Heated Room D with Clay Layers Compared with Field Data

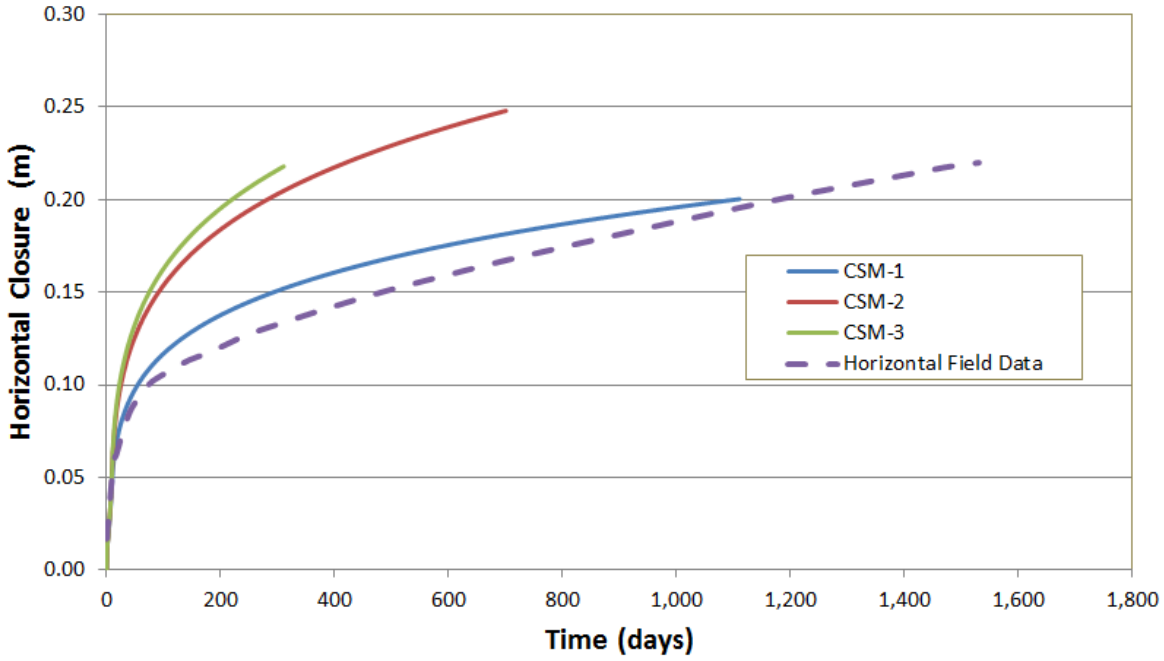

Figure 2-11. Horizontal Closure History for Heated Room D with Clay Layers Compared with Field Data

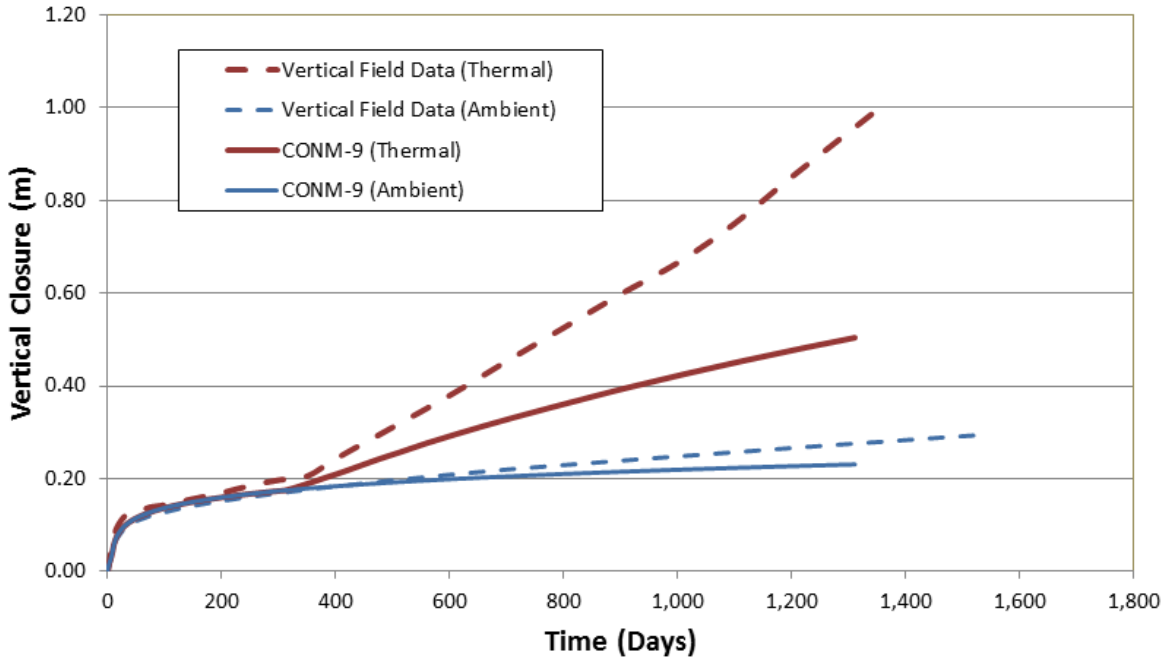

Figure 2-12. Vertical Closure History for Heated Room B (CONM-11, Thermal) Compared with Field Data and Room D (CONM-Ambient)

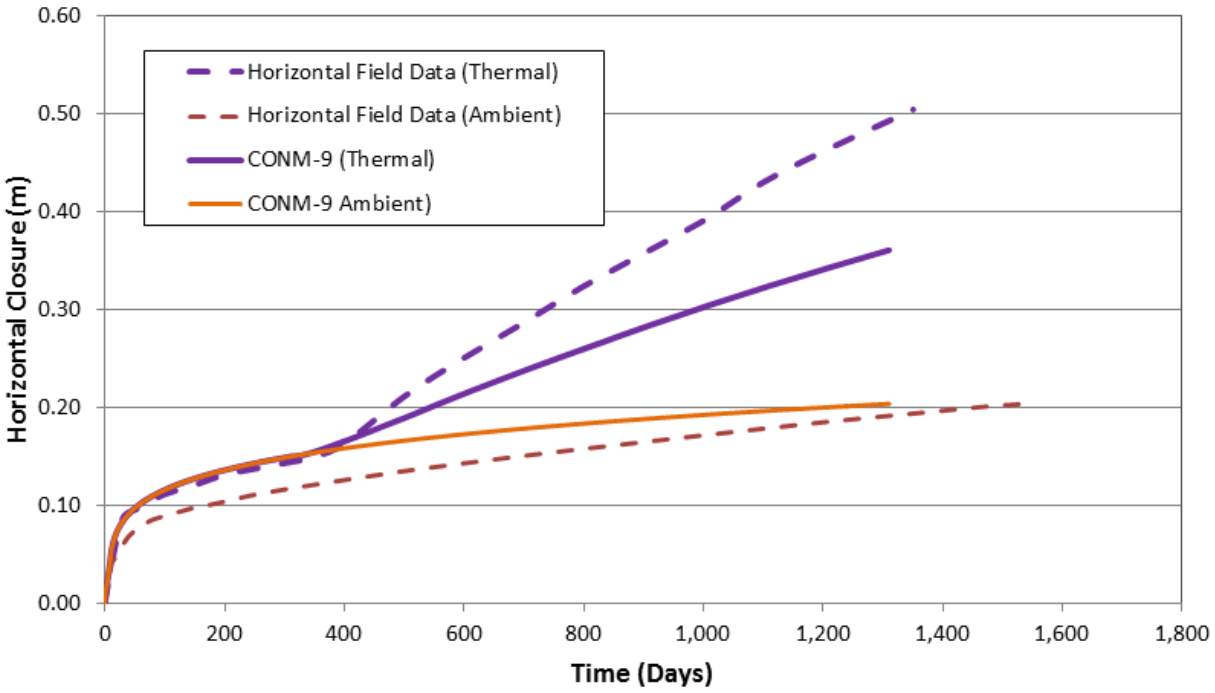

Figure 2-13. Horizontal Closure History for Heated Room B (CONM-11, Thermal) Compared with Field Data and Room D (CONM-Ambient)

3 CONCLUSIONS

This report describes results of numerical simulations of in situ experiments at the WIPP site using the geomechanics modeling computer code FLAC with a user-defined material model that includes elastic, plastic, and creep deformations as described in Chapter 1. The simulations were performed to evaluate approaches to modeling salt rock mechanical behavior in underground openings. Simulations were performed for ambient conditions (Room D) to evaluate approaches to material modeling and for heated conditions (Room B) to evaluate thermal effects. Room D and Room B have the same geometry and closely similar geologic conditions (Rath and Argüello, 2012). Two models of the host rock were used in the study: (1) a continuum model with uniform mechanical and thermal properties and (2) a discontinuum model in which clay seams were explicitly incorporated as horizontal interfaces, with uniform mechanical and thermal rock properties between the interfaces. For evaluating the performance of the models, calculated vertical and horizontal convergences of the room openings were compared with collected field data.

3.1 Host Rock as Continuum

Ofoegbu and Dasgupta (2017) compared convergence of the openings calculated using models based on coupled creep and plasticity with models based on creep only. The coupled model showed improvements in the shape of the calculated convergence history and the magnitude of calculated convergence improved to approximately 75 percent of the measured convergence approximately 1,300 days after excavation. In this report a series of parametric studies were performed on the choices of transient creep parameters (a_0, a_1, and a_2) and the horizontal to vertical stress ratio (σ_h/σ_v) that provide a close match to the field measurements. As shown in Table 2-1, the creep parameter a_0 was varied from 0.008 to 0.05; only two values of a_1, 1,750 and 2,000, were used; and a_2 was kept constant at 0.375. Rath and Argüello (2012) assumed the stress ratio to be 1.0, but in situ stress measurements at the WIPP excavation horizon were not available to verify the assumption. In this study, the stress ratio was varied between 1.0 to 1.5. Results of the 11 simulation cases shown in Figures 2-4 and 2-5 were narrowed to three cases—CONM-7, -9, and -11—that compared well with the field data (see Figures 2-9 and 2-10). Simulation results for Room D show the magnitudes and trends of the calculated convergence with time are similar to the measured convergence. However, the shapes of the calculated convergence histories are different from the shape of the measured history, especially for longer times. Model convergence histories may be improved to better match the measured convergence histories by: (i) modifying values of the plasticity model parameters and (ii) developing a model to represent the effects of plastic deformation on the creep parameters as described in Section 3.4.1.

3.2 Effect of Clay Seams

Deformation of clay seams or clayey interfaces between salt rock layers could contribute to overall rock behavior around the openings. One approach to account for deformation of clay seams was evaluated by explicitly representing the seams as contact surfaces using the interface feature in FLAC. Although this is a potential improvement, interface parameters of the clay seams need to be calibrated in order to match the measured convergence. In this approach, potential creep in the clay seams is not included. The clay seams can be modeled as thin layers instead of interfaces and a material model based on coupled creep and plasticity can be applied. In addition, response of clay seams under heated conditions would be represented better by modeling the clay seams as thin layers. Reedlunn (2016) suggested development of a

constitutive model for clay seam material based on a laboratory test program and model validation based on underground in situ tests.

3.3 Thermal Effects

For the thermal simulation of Room B, model parameters for analysis case CONM-9 were used. The history plots for calculated convergence show an increase in convergence with application of thermal loading after the ambient period, consistent with the measured convergence history. However, during the period of heating, the calculated magnitudes for both vertical and horizontal convergence were smaller than the measured magnitude. The model results for horizontal closure were better than those for vertical closure. The authors expect that the accuracy of the calculation can be improved, as discussed in Section 3.4.2.

3.4 Material Model Modifications to Improve Accuracy of Calculated Behavior

The model results led to the identification of potential modifications in material modeling that may lead to better understanding of salt rock behavior around heated openings. The modifications described in the following subsections should improve the coupling of creep and plastic deformation modeling and thermal-mechanical coupling.

3.4.1 Coupling of Creep and Plastic Deformations

In the material model used for the simulations, creep and plastic deformations are coupled through deviatoric stress. Creep rates are proportional to a power function of deviatoric stress, while plastic deformations are driven by deviatoric stress. Both plastic and creep deformations cause the deviatoric stress to decrease. The coupling of plastic and creep deformation, which is dependent on a decrease in deviatoric stress, appears to be weak.

The strength of coupling of the two deformation mechanisms could be increased by representing the controlling parameters as functions of distortional strain. Both creep and plastic deformations contribute to distortional strain—at times, as observed in the model, in comparable magnitudes—such that properties dependent on distortional strain will be affected by each deformation mechanism. The modeled shear resistance varies with distortional strain as defined through the plasticity model parameters. However, a similar model of the creep resistance needs to be developed by modeling the creep parameters as functions of distortional strain. The resulting model will account for any feedback mechanism to increase or decrease the deformation rates and can be used effectively to match the measured convergence and hence evaluate the effects of the creep and plasticity model parameters.

3.4.2 Thermal and Mechanical Coupling

Thermal changes affect mechanical deformation through increased stress due to suppressed thermal expansion. The mechanical effects of thermal loading depend on the temperature and property gradients, mechanical boundary conditions, and thermal expansivity. These effects are well understood and are represented in the thermal modeling. However, additional thermal effects could result from thermal strain affecting mechanical behavior, such as through dilation-dependent bulk modulus or other parameters dependent on distortional strain. The approach to representing the effects of thermal strain on mechanical property needs additional investigation, because thermal effects on dilation and distortional strain are not defined explicitly.

4 REFERENCES

Desai, C.S. and H.J. Siriwardane. "Constitutive Laws for Engineering Materials with Emphasis on Geologic Materials." Englewood Cliffs, New Jersey: Prentice-Hall, Inc. 1984.

European Commission. "Compilation of Existing Constitutive Models and Experimental Field or Laboratory Data for the Thermal-Hydraulic (THM) Modelling of the Excavation Disturbed Zone (EDZ) in Rock Slat." Sixth Framework Programme. EURATOM Radioactive Waste Management. THERESA Project. Work Package 3 Deliverable 5. 2007.

Hunsche U. and A. Hampel. "Rock Salt—the Mechanical Properties of the Host Rock Material for a Radioactive Waste Repository." *Engineering Geology*. Vol. 52. pp. 271–291. 1999.

Itasca Consulting Group, Inc. "FLAC Fast Lagrangian Analysis of Continua." Version 8. Minneapolis, Minnesota: Itasca Consulting Group, Inc. 2016.

Ofoegbu, G. and B. Dasgupta. "Implementation of a Creep Model in FLAC to Study the Thermomechanical Response of Salt as a Host Repository Medium—2nd Progress Report." San Antonio, Texas: Center for Nuclear Waste Regulatory Analyses. 2017.

Ofoegbu, G. and B. Dasgupta. "Implementation of a Creep Model in FLAC to Study the Thermomechanical Response of Salt as a Host Repository Medium—Progress Report." San Antonio, Texas: Center for Nuclear Waste Regulatory Analyses. 2015.

Rath, J.C. and J.G. Argüello. "Revisiting Historic Numerical Analyses of the Waste Isolation Pilot Plant (WIPP) Room B and D *In-Situ* Experiments Regarding Thermal and Structural Response." SAND20–12–7525. Albuquerque, New Mexico: Sandia National Laboratories. 2012.

Reedlunn, B. "Reinvestigation into Closure Predictions of Room D at the Waste Isolation Pilot Plant." SAND2016-9961. Albuquerque, New Mexico: Sandia National Laboratories. 2016.